Self-Induced Glassy Phase in Multimodal Cavity Quantum Electrodynamics

V. Erba,[1,2,*] M. Pastore,[1,2,3] and P. Rotondo[1,2]
[1]Dipartimento di Fisica dell' Università degli Studi di Milano, via Celoria 16, 20100 Milano, Italy
[2]Istituto Nazionale di Fisica Nucleare, sezione di Milano, via Celoria 16, 20100 Milano, Italy
[3]Universit Paris-Saclay, CNRS, LPTMS, 91405 Orsay, France

(Received 6 January 2021; accepted 5 April 2021; published 3 May 2021)

We provide strong evidence that the effective spin-spin interaction in a multimodal confocal optical cavity gives rise to a self-induced glassy phase, which emerges exclusively from the peculiar Euclidean correlations and is not related to the presence of disorder as in standard spin glasses. As recently shown, this spin-spin effective interaction is both nonlocal and nontranslational invariant, and randomness in the atoms' positions produces a spin glass phase. Here we consider the simplest feasible disorder-free setting, where atoms form a one-dimensional regular chain and we study the thermodynamics of the resulting effective Ising model. We present extensive results showing that the system has a low-temperature glassy phase. The model depends on the adimensional parameter $\alpha = (a/w_0)^2$, a being a lattice spacing and w_0 an interaction length scale. Notably, for rational values of $\alpha = p/q$, the number of metastable states at low temperature grows exponentially with q and the problem of finding the ground state rapidly becomes computationally intractable, suggesting that the system develops high-energy barriers and ergodicity breaking occurs.

DOI: 10.1103/PhysRevLett.126.183601

Cavity quantum electrodynamics (CQED) provides—together with trapped ions [1,2], circuit [3], and waveguide QED [4]—one of the state-of-the-art controllable platforms for quantum simulation. In a first series of experiments [5,6], it was shown that Bose-Einstein condensates (BECs) in single-mode optical cavities undergo an abrupt change from a dark to a superradiant state, which is the nonequilibrium counterpart of the phase transition predicted by Hepp and Lieb (HL) [7–11] within their exact statistical physics analysis of the Dicke model.

More recently, a setting where the optical cavity sustains many degenerate electromagnetic modes was explored [12]. Here, the physics arising from the interaction of the many modes with the atoms in random positions is much richer than the one observed in the single-mode case [13–15]: first, frustration (generated by the random positions of the atoms in the cavity) may lead to a glassy behavior; second, the form of the effective spin-spin couplings is reminiscent of the interaction arising from Hebbian learning in the so-called Hopfield model [16], which describes the simplest way to obtain an associative memory.

This discovery led the authors of Refs. [17,18] to investigate the equilibrium statistical physics of the full quantum disordered Dicke model with M degenerate electromagnetic modes, by generalizing the original work by HL. This analysis allowed them to establish that, in the strong coupling limit, the energy landscape shares the same structure of minima of the Hopfield model, i.e., a ferromagnetic landscape with M degenerate ground states corresponding to the stored memory patterns. Whether this picture survives to the interaction with an environment has been the subject of subsequent work [19–22].

The feasibility of a quantum optical-based associative memory has been investigated in a series of papers by Lev and co-workers [23–25]. Here the authors proved that the effective spin-spin interaction can be sign changing with a tunable range and identified a protocol to implement associative memories in CQED [26].

More importantly, they were able to obtain the specific form of the interaction for confocal cavities [26], showing explicitly its nonlocal and nontranslational invariant nature (in fact, it depends on the scalar product of the positions of two atoms). Understanding the physics arising by this peculiar spin-spin interaction is a challenge by itself, since taking into account Euclidean correlations is commonly a hard task in statistical physics.

Our goal in this Letter is to shed light on the spin-spin interaction arising in multimodal optical cavities by revealing an exotic spin glass phase that appears at low temperature *without* any explicit quenched disorder in the Hamiltonian. We consider the simplest feasible setting: atoms lie on a regular one-dimensional chain, collinear with the main axis of the optical cavity. In this case, the energy depends on a single adimensional parameter α. For rational $\alpha = p/q$, the interaction is periodic and we show that the free-energy landscape is a q-dimensional manifold. Surprisingly, as q grows, we observe an exponential proliferation of metastable states, which is typical of disordered systems with a complex free-energy landscape.

Our analysis shows that in multimodal CQED the presence of disorder in the atomic positions is not fundamental to achieve such a rough landscape. More formally, this physical system provides an explicit realization of self-induced quenched disorder as introduced in Refs. [27–29]. This emerging feature and its relation to frustration have been investigated also in models at finite connectivity [30,31] and is expected to play a role in the understanding of the low-temperature phase of structural glasses [32].

The model.—We consider an Ising model with energy $E(\boldsymbol{\sigma}) = \frac{1}{2N}\sum_{i,j=0}^{N-1} J_{ij}\sigma_i\sigma_j$, where the σ_i's are binary ± 1 variables and the couplings depend on the positions $\mathbf{r}_i$ of the atoms in the cavity as

$$J_{i,j} = \cos\left(2\pi \frac{\mathbf{r}_i \cdot \mathbf{r}_j}{w_0^2}\right), \tag{1}$$

where the length scale w_0 is proportional to the width of the Gaussian fundamental transverse mode. This form of the effective spin-spin interaction has been derived in detail in Refs. [23–25]. In [26] the authors investigated, mostly with numerical methods, the properties of the resulting energy landscape, focusing on the case where atoms were in random positions. Here we consider a disorder-free scenario where atoms form a one-dimensional lattice; i.e., the mth atom is in position $\mathbf{r}_m = a(m - L)\hat{\mathbf{n}}$ where a is the lattice spacing, $L = N/2$, and $\hat{\mathbf{n}}$ is a unit vector orthogonal to the cavity mirrors and origin at the center of the cavity. This choice implies that the Lth atom lies at the origin of the chain; since the interaction is nontranslationally invariant, other conventions may qualitatively change the physics of the system (see Supplemental Material for more details [33]). Notice that the couplings in Eq. (1) depend on a single adimensional parameter $\alpha = (a/w_0)^2$, which in the experimental proposal [26] can be manipulated acting on the positions of the BEC ensembles (the effective Ising spins of the present model) via optical tweezers.

Variational free energy of the system.—Our first goal is to investigate the thermodynamics of the Ising model with couplings given by Eq. (1) by looking at its free-energy $f = -1/(N\beta)\log Z$, where $\beta = 1/T$ is the inverse of the temperature T and $Z = \sum_{\boldsymbol{\sigma}} e^{-\beta E(\boldsymbol{\sigma})}$ is the partition function. We stress that the thermodynamic temperature T that we introduce here is not the real temperature of the experimental implementation of the model. In fact, in [26] it is proven that the relaxation dynamics of the system is a steepest descent dynamics in the free-energy landscape at null thermodynamic temperature T. For this reason, we will focus on the case $T = 0$ in the main text, and we will discuss the high-temperature phase in the Supplemental Material [33].

Analytical progress can be made for rational $\alpha = p/q$, where p and q are coprime positive integers. For irrational α, it is reasonable to expect that studying the rational approximation obtained by truncating the continued fraction expansion of α may deliver insights on the physics of the model, as it occurs, for instance, in Ising systems with long-range repulsion [34,35] or in the Frenkel-Kontorova model [36].

The strategy to compute the partition function of the model at rational $\alpha = p/q$ is as follows: since the interaction is periodic with period q, it is convenient to introduce q collective variables m_r $(r = 0, 1, \ldots, q-1)$, which represent the magnetizations on the sublattices $\Lambda_r = \{iq + r, i = 0, 1, \ldots, 2\ell - 1\}$ (where for simplicity, $L = \ell q$), i.e., $m_r = 1/(2\ell)\sum_{i=0}^{2\ell-1}\sigma_{iq+r}$ (see also Fig. 1). Notice that $|m_r| \leq 1\ \forall\ r = 0, 1, \ldots, q-1$. This choice of grouping the microscopic variables allows us to write the energetic contribution to the partition function as [33]

$$E(\{m_r\}) = \frac{\ell}{q}\sum_{r,s=0}^{q-1}\cos\left(\frac{2\pi p}{q}rs\right)m_r m_s. \tag{2}$$

The reduced $q \times q$ interaction matrix is depicted in Fig. 1 for two different values of $\alpha = p/q$. The entropic

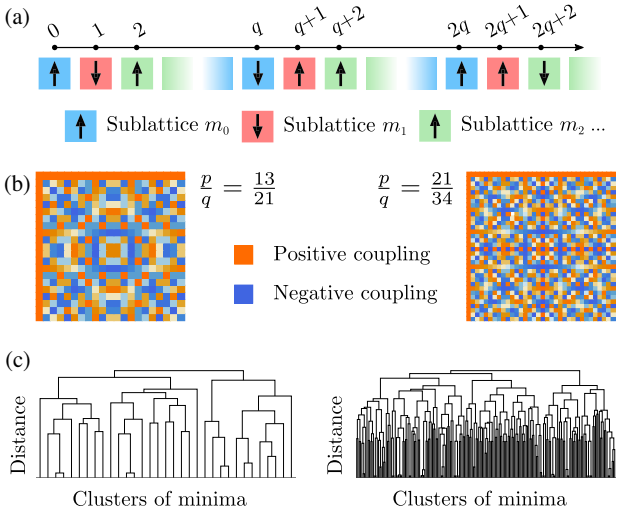

FIG. 1. Collective variables, reduced interaction matrix, and proliferation of metastable states increasing q. (a) Identification of the collective variables to study the partition function analytically. Since the interaction is periodic, it is natural to group spins lying on the sublattices $\Lambda_r = \{iq + r, i = 0, 1, \ldots, 2\ell - 1\}$. In this way, we can define q mesoscopic magnetizations m_r with $r = 0, 1, \ldots, q-1$ and reduce the partition function to an integral over these q variables. (b) Reduced $q \times q$ interaction matrix for two different values of $\alpha = p/q$. Removing the first row and column, the resulting $(q-1) \times (q-1)$ matrix displays a reflection symmetry around the antidiagonal, which allows us to further reduce the dimensionality of the free-energy manifold from q to $\lfloor q/2 + 1 \rfloor$. (c) Schematic representation by hierarchical clustering of the energy landscape at the two different values of $\alpha = 13/21, 21/34$. We obtain this representation by displaying the local minima of the energy in Eq. (2) as the leaves of a dendrogram. Distance is increasing along the vertical axis and pairs of distinct clusters at distance d (measured from their center) are iteratively joined together in a new node at height d. As q increases, we observe a proliferation of local minima.

contribution can be obtained as well by counting the degeneracy of each magnetization m_r, i.e., how many microscopic spin configurations contribute to a given value of the magnetization. In the thermodynamic limit, we can easily estimate this entropy as

$$S(\{m_r\}) = 2\ell\left[q\log 2 - \sum_{\sigma=\pm 1}\sum_{s=0}^{q-1}\frac{1+\sigma m_s}{2}\log(1+\sigma m_s)\right]. \tag{3}$$

In conclusion, the variational free-energy density in the thermodynamic limit is given by

$$f(\{\tilde{m}_r\}) = 1/(2\ell q)[E(\{\tilde{m}_r\}) + 1/\beta S(\{\tilde{m}_r\})] \tag{4}$$

and the actual free energy of the system at equilibrium is obtained by finding the global minimum $\tilde{\mathbf{m}}^* = (\tilde{m}_0^*, \tilde{m}_1^*, \ldots, \tilde{m}_{q-1}^*)$ of this q-dimensional function. Interestingly, we can further reduce the dimensionality of the problem from q to $\lfloor q/2+1 \rfloor$ by exploiting the symmetry under reflection around the antidiagonal of the $(q-1)\times(q-1)$ interaction matrix obtained by removing the first row and column of the original reduced matrix (see also Fig. 1 and Supplemental Material [33]). This reduction is crucial for numerical simulations, as it halves the number of effective degrees of freedom of the model.

Exponential number of metastable states at $T=0$.—To characterize the $T=0$ behavior of the model, we start by focusing our attention on the enumeration of the metastable states, i.e., local minima of the energy in Eq. (2). As a first point, we observe a proliferation of the local minima of the energy in Eq. (2) when we increase q. This phenomenon is shown for two different values of α in Fig. 1(c), where we exhibit a representation of the energy landscape based on hierarchical clustering (see Fig. 1 for a more detailed explanation). Note that, at variance with the usual spin glass picture, where the number of metastable states diverges in the thermodynamic limit, in the present case this number is strictly finite as long as also q is fixed, and the glassy behavior is observed only at large q. In the following, we numerically characterize the scaling of the number of metastable states with q.

Again our strategy is to probe the energy landscape by performing many gradient descents starting from a very large number of different initial conditions sampled uniformly on the q-dimensional hypercube $|\tilde{m}_r| \leq 1\ \forall\ r = 0, 1, \ldots, q-1$ and to count the total number of different local minima identified in this way. This algorithm presents two obvious drawbacks: (i) it may fail in finding the local minima of Eq. (4) with very narrow basins of attraction and (ii) for large q it may systematically underestimate the number of local minima if this is growing exponentially, since the number of initial conditions we need to probe the landscape also grows exponentially in q. Thus, our algorithm provides a lower bound to the number of local minima at fixed q and may in any case systematically miss those minima with extremely narrow basins of attraction. As a consequence, we need to pay particular attention to understand whether the estimate of the local minima at a given q we obtain is reliable or not, i.e., if the lower bound we provide is strict or not.

An effective method to check whether at a given q we have exhaustively found most of the local minima of the landscape is to monitor the number of distinct minima found as a function of the number of gradient descents performed [see insets in Fig. 2(a)]. In this way, we can immediately argue whether the estimate is reliable by looking at how close we are to saturation. It turns out that $\sim 10^5$ gradient descents are sufficient below $q \simeq 60$, whereas one should increase this number by at least one order of magnitude for $q > 60$, and this is beyond our computational power.

Our results for the scaling of the number of local minima $N_{\min}$ as a function of q are shown in Fig. 2(a): in the regime where the estimate is reliable (up to values of $q \simeq 60$), we find an exponential proliferation of metastable states of the form $N_{\min} \sim b^q$ with $b \simeq 1.16$.

We also computed the average linear size of the basins (defined as the average distance between a minimum and the furthest starting point leading to said minimum under gradient descent), which is relevant for the application to associative memories [26]. We found that these basins are extensive in the thermodynamic limit; i.e., they occupy a finite volume of the phase space, and their linear size grows with q as q^c with $c \simeq 0.37$.

Self-induced quenched disorder in CQED.—The exponential scaling of the number of local minima, which is similar to the one observed in spin glass models [37], is due to the competition of ferromagnetic and antiferromagnetic couplings in the Hamiltonian of the model, leading to frustration. However, this result alone does not guarantee that the energy landscape of our model is complex. Indeed, it is well known that frustrated Hamiltonians of Ising spins may display an exponential number of degenerate ground states without exhibiting a spin glass phase, i.e., without extensive energy barriers, as in the case of the antiferromagnetic Ising model on the triangular lattice.

A significant hint suggesting that the model has a true glassy phase is given by the computational complexity of the problem of finding the ground state. In fact, another interesting feature of many genuine spin glass models with complex energy landscapes is that finding their ground state is a nondetermistic polynomial-time hard problem (NP-hard problem) (intuitively this means that the computational complexity of this optimization problem grows exponentially with the system size): this is true, for instance, for the Sherrington-Kirkpatrick (SK) and for the $p > 2$-spin Ising or spherical models [38,39] or for the k-satisfiability problem [40]. Let us consider the effective energy in Eq. (2): here we have to minimize a quadratic function of q magnetizations on the domain

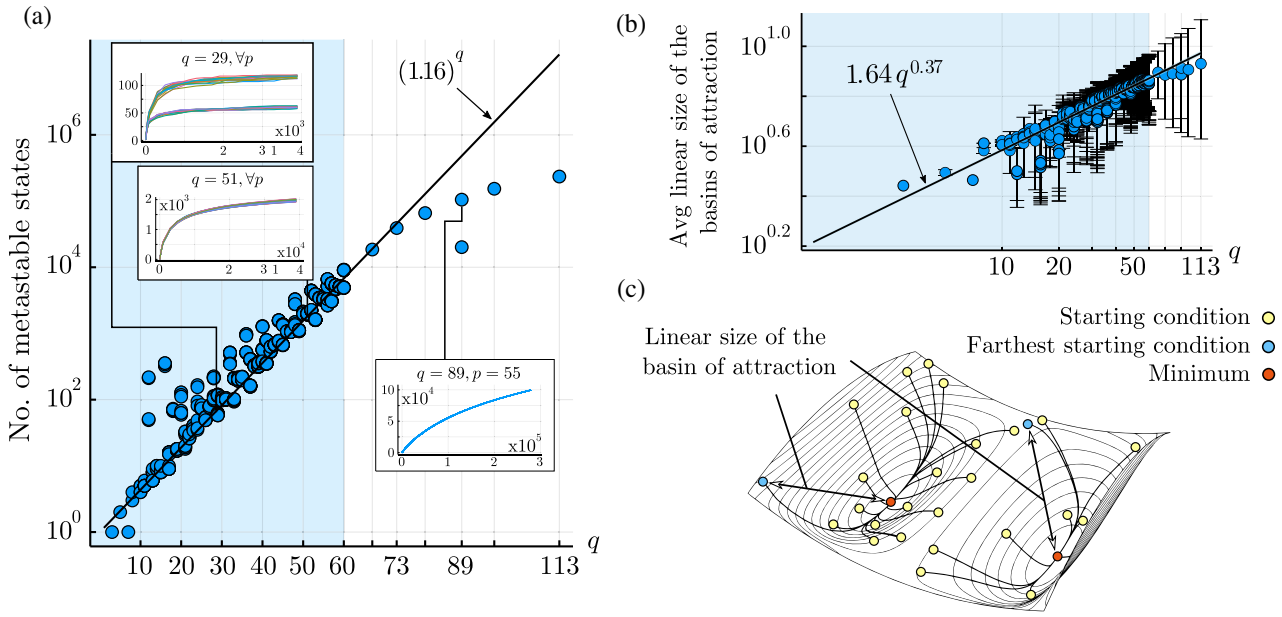

FIG. 2. Exponential number of metastable states increasing q. (a) Scaling of the number of local minima of the energy in Eq. (2) as a function of q (different values of p are shown for each value of q; see Supplemental Material [33]). To check whether at a given q the estimate of the number of metastable states is reliable, in the insets we display the number of distinct minima found as a function of the number of gradient descents attempted for three representative values of q. The closer we are to saturation, the more accurate is the estimate. Above $q \sim 60$ the estimate is not reliable, since we are missing a large number of minima (see right inset). The log-linear scale of the main plot highlights the exponential growth below $q \sim 60$, where the estimate is reliable (see left insets). (b) The average linear size of the basins of attraction at fixed $\alpha = p/q$ grows algebraically with q as $q^{0.37}$. Error bars denote one sample variance. (c) The linear size of a given basin of attraction is measured by collecting all the initial conditions that flow to a given minimum and keeping as the linear size the distance between the minimum and the farthest initial condition from it.

$|\tilde{m}_r| \; \forall \; r = 0, 1, \ldots, q-1$. In computer science, this is called a "quadratic programming" problem [41,42] and its computational complexity depends on whether the corresponding quadratic form is positive definite or not. In particular, the problem is NP hard if the quadratic form has at least one negative eigenvalue [43]. In the case of Eq. (2), it is possible to show that the reduced interaction matrix $J_{rs} = \cos(2\pi prs/q)$ has at least one negative eigenvalue for any q (see Supplemental Material [33]).

Even the NP-hard nature of the problem of finding the ground state of a given model is not necessarily a symptom of a complex free-energy landscape. Indeed, the theory of computational complexity deals with the *worst-case* scenario, whereas thermodynamic properties as the free energy provide information on the *typical* behavior of the system. As such, it may be that worst-case instances of a NP-hard problem have zero measure with respect to the probability distribution of the couplings and/or disorder. In our specific case, we explicitly observed an exponential scaling of the time needed to find the GS of the system using a state-of-the-art generic quadratic programming optimizer (see Fig. 3), suggesting that the problem under consideration is indeed a worst-case instance, and that the model has a low-temperature glassy phase.

This last observation allows us to highlight a crucial difference between spin-spin interaction in multimodal CQED and systems such as the SK model: in most spin glasses, the number of random couplings grows with the size of the system [e.g., in the SK model, we need to specify $N(N-1)/2$ parameters at size N]. On the contrary, the Ising model we have studied does not contain explicitly any quenched disorder, and only the parameter α has to be specified at any size N. Only a few spin models exhibiting a complex free-energy landscape without quenched disorder

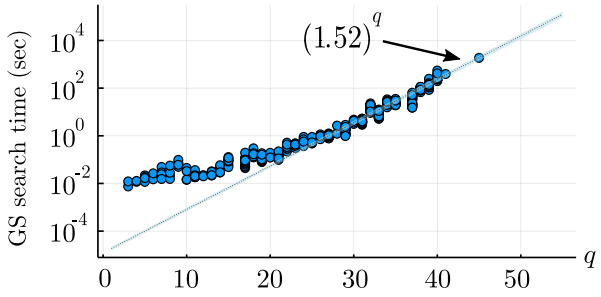

FIG. 3. The run time for the ground-state search problem scales exponentially with q. Scaling of the run time of the ground-state (GS) search performed using a state-of-the-art optimizer (IBM CPLEX [44,45]) as a function of q (again, different values of p are shown for each value of q). Up to $q = 45$, the run time scales exponentially with q, suggesting that the GS search problem is a worst-case instance of nonpositive-definite quadratic programming.

exist in the literature [27–29]. These systems have been studied extensively in the past, since they are considered toy models of the glass transition, where disorder is self-induced and not present at the level of the Hamiltonian. Note that interaction in confocal CQED provides an explicit physical realization (up to a rescaling of the coupling constants and boundary terms) of the cosine model introduced in Ref. [46], if one chooses $p = 1$ and $q = N$.

Discussion and outlooks.—The investigation of self-induced glassy phases in confocal CQED presents one major advantage over traditional solid-state systems: the experimental setup is highly controllable. The interaction can be tuned by manipulating the atoms' positions and the spin states can be probed by holographic imaging [23], in contrast with standard spin glasses where the system is dirty and quite difficult to probe. Another relevant aspect concerns the typical timescales of the glassy dynamics in this proposed quantum-optical setup. In typical realizations of spin or structural glasses in condensed matter, the interaction among degrees of freedom is mediated, respectively, by conduction electrons or by intermolecular forces, while in this quantum-optical proposal it is carried by photons: this may lead to a speed-up of the glassy dynamics due to a faster spin-flip rate. However, this is a speculative argument and a more detailed analysis of the typical timescales of this complex system is needed to substantiate this intuition.

The authors are grateful to Giacomo Gradenigo for the useful remarks and discussions. P. R. acknowledges funding by the INFN Fellini program H2020-MSCA-COFUND Grant Agreement No. 754496.

*Corresponding author.
vittorio.erba@posteo.net

[1] J. I. Cirac and P. Zoller, Phys. Rev. Lett. **74**, 4091 (1995).
[2] D. Leibfried, R. Blatt, C. Monroe, and D. Wineland, Rev. Mod. Phys. **75**, 281 (2003).
[3] A. Blais, R.-S. Huang, A. Wallraff, S. M. Girvin, and R. J. Schoelkopf, Phys. Rev. A **69**, 062320 (2004).
[4] H. Zheng, D. J. Gauthier, and H. U. Baranger, Phys. Rev. Lett. **111**, 090502 (2013).
[5] K. Baumann, R. Mottl, F. Brennecke, and T. Esslinger, Phys. Rev. Lett. **107**, 140402 (2011).
[6] K. Baumann, C. Guerlin, F. Brennecke, and T. Esslinger, Nature (London) **464**, 1301 (2010).
[7] K. Hepp and E. H. Lieb, Ann. Phys. (N.Y.) **76**, 360 (1973).
[8] K. Hepp and E. H. Lieb, Phys. Rev. A **8**, 2517 (1973).
[9] C. Emary and T. Brandes, Phys. Rev. E **67**, 066203 (2003).
[10] C. Emary and T. Brandes, Phys. Rev. Lett. **90**, 044101 (2003).
[11] D. Nagy, G. Kónya, G. Szirmai, and P. Domokos, Phys. Rev. Lett. **104**, 130401 (2010).
[12] S. Gopalakrishnan, B. L. Lev, and P. M. Goldbart, Nat. Phys. **5**, 845 (2009).
[13] S. Gopalakrishnan, B. L. Lev, and P. M. Goldbart, Phys. Rev. Lett. **107**, 277201 (2011).
[14] P. Strack and S. Sachdev, Phys. Rev. Lett. **107**, 277202 (2011).
[15] S. P. Kelly, A. M. Rey, and J. Marino, Phys. Rev. Lett. **126**, 133603 (2021).
[16] J. J. Hopfield, Proc. Natl. Acad. Sci. U.S.A. **79**, 2554 (1982).
[17] P. Rotondo, M. Cosentino Lagomarsino, and G. Viola, Phys. Rev. Lett. **114**, 143601 (2015).
[18] P. Rotondo, E. Tesio, and S. Caracciolo, Phys. Rev. B **91**, 014415 (2015).
[19] E. Fiorelli, M. Marcuzzi, P. Rotondo, F. Carollo, and I. Lesanovsky, Phys. Rev. Lett. **125**, 070604 (2020).
[20] E. Fiorelli, P. Rotondo, F. Carollo, M. Marcuzzi, and I. Lesanovsky, Phys. Rev. Research **2**, 013198 (2020).
[21] P. Rotondo, M. Marcuzzi, J. P. Garrahan, I. Lesanovsky, and M. Mller, J. Phys. A **51**, 115301 (2018).
[22] F. Carollo and I. Lesanovsky, arXiv:2009.13932.
[23] Y. Guo, R. M. Kroeze, V. D. Vaidya, J. Keeling, and B. L. Lev, Phys. Rev. Lett. **122**, 193601 (2019).
[24] Y. Guo, V. D. Vaidya, R. M. Kroeze, R. A. Lunney, B. L. Lev, and J. Keeling, Phys. Rev. A **99**, 053818 (2019).
[25] V. D. Vaidya, Y. Guo, R. M. Kroeze, K. E. Ballantine, A. J. Kollár, J. Keeling, and B. L. Lev, Phys. Rev. X **8**, 011002 (2018).
[26] B. P. Marsh, Y. Guo, R. M. Kroeze, S. Gopalakrishnan, S. Ganguli, J. Keeling, and B. L. Lev, arXiv:2009.01227.
[27] J. Bernasconi, J. Phys. II (France) **48**, 559 (1987).
[28] E. Marinari, G. Parisi, and F. Ritort, J. Phys. A **27**, 7615 (1994).
[29] J. P. Bouchaud and M. Mézard, J. Phys. I (France) **4**, 1109 (1994).
[30] J. Villain, J. Phys. C **10**, 1717 (1977).
[31] M. Yosefin and E. Domany, Phys. Rev. B **32**, 1778 (1985).
[32] G. Parisi, P. Urbani, and F. Zamponi, *Theory of Simple Glasses: Exact Solutions in Infinite Dimensions* (Cambridge University Press, Cambridge, England, 2020).
[33] See Supplemental Material at http://link.aps.org/supplemental/10.1103/PhysRevLett.126.183601 for more details on the computations and on the numerical simulations presented in the main text.
[34] P. Bak and R. Bruinsma, Phys. Rev. Lett. **49**, 249 (1982).
[35] P. Rotondo, L. G. Molinari, P. Ratti, and M. Gherardi, Phys. Rev. Lett. **116**, 256803 (2016).
[36] S. Aubry and P. Le Daeron, Physica (Amsterdam) **8D**, 381 (1983).
[37] M. Mézard, G. Parisi, and M. A. Virasoro, *Spin Glass Theory and Beyond* (World Scientific, Singapore, 1986).
[38] E. Gardner, Nucl. Phys. **B257**, 747 (1985).
[39] F. Barahona, J. Phys. A **15**, 3241 (1982).
[40] M. Mézard, G. Parisi, and R. Zecchina, Science **297**, 812 (2002).
[41] S. Mertens, Comput. Sci. Eng. **4**, 31 (2002).
[42] M. Mezard and A. Montanari, *Information, Physics, and Computation* (Oxford University Press, New York, 2009).
[43] P. M. Pardalos and S. A. Vavasis, J. Global Optim. **1**, 15 (1991).
[44] IBM, CPLEX 12.10, User's Manual for CPLEX (2020), https://www.ibm.com/docs/en/SSSA5P_12.8.0/ilog.odms.studio.help/pdf/usrcplex.pdf.
[45] I. Dunning, J. Huchette, and M. Lubin, SIAM Rev. **59**, 295 (2017).
[46] E. Marinari, G. Parisi, and F. Ritort, J. Phys. A **27**, 7647 (1994).